The effect of cytochrome c on the melting transition of charged model lipid-membranes using FTIR-spectroscopy

Klaus Bruun Pedersen
110383-xxxx

June 8th 2007

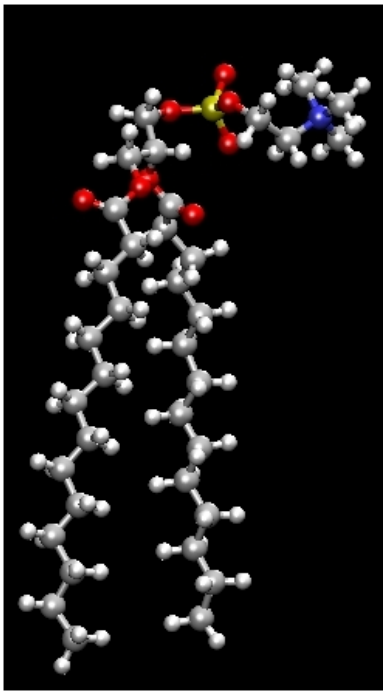

Bachelor Project
Membrane Biophysics and Thermodynamics Group
Niels Bohr Institute
University of Copenhagen

Supervisers: Thomas Heimburg
Matthias Fidorra

Abstract

The biological membrane has historically never played a very dominant role in biochemistry. It has merely been conceived as a barrier that hinds the cellinteriors from diffusing. In *Hodgkin and Huxley*'s model of nerve signaling it works as a capaciter.
In this thesis I examine the effect of the peripheral protein cytochrome c on a membrane consisting of the charged lipid DMPG.
I will show that the heatcapacity of the membrane as a function of temperature is changed with the addition of cytochrome c. The heatcapacity peaks around the meltingpoint for the membrane but the peak of the heatcapacity is lowered, broadened and shifted to a higher temperature when cytochrome c i added. Hence the meltingpoint is altered.
The approach of this thesis is thermodynamical and the measurements are with FTIR-spectroscopy.

Resumé

Biologiske membraner har historisk set aldrig spillet en central rolle i biokemien. Den er blevet opfattet som en barriere, der skulle forhindre cellens dele i at difundere væk. I *Hodgkin and Huxley*'s model for nervesignalering fungerer den som en capacitor.
I denne opgave vil jeg undersøge hvordan overfladeproteinet cytochrom c indvirker på en membran bestående af den ladede lipid DMPG.
Jeg vil vise at varmekapaciteten af en membran som funktion af temperaturen ændrer sig når der er cytochrome c på den. Varmekapaciteten topper når membranen smelter men kurven bliver lavere, bredere og forskubbes til en højere temperatur når cytochrome c bliver tilsat. Derved er også smeltepunktet forskudt. Tilgangen i denne opgave er termodynamisk og forsøgene er udført ved FTIR-spektroskopi.

Acknowledgements

I would like to thank Matthias Fidorra for his advice and for supplying me with software to make my data analysis much easier.
Further I would like to thank Thomas Heimburg for support and guidance, the Membrane Crew of NBI for helping me in the lab and Myself for keeping me company through the endless hours by the FTIR-spectrometer - without company I would surely have gone mad.

Contents

1 Introduction **4**

1.1 Motivation . . . 4

1.2 The cell . . . 4

1.3 Biomembranes . . . 4

1.3.1 The lipids . . . 5

1.3.2 Proteins . . . 7

1.3.3 The melting of the biomembrane . . . 8

1.4 Cooperativity and domain formation . . . 10

1.5 The role of anaesthetics . . . 10

1.6 Neurons and nerve pulses . . . 12

2 Materials and methods **13**

2.1 FTIR-spectroscopy . . . 13

2.1.1 Peakpositioning and generating a meltingprofile . . . 14

2.2 Sample preparation . . . 17

2.2.1 The chamber . . . 18

2.3 Samples in deuterated water . . . 19

2.4 Estimate of errors . . . 19

2.4.1 Temperature calibration . . . 19

3 Theory **21**

3.1 The meltingpoint of a homogeneous membrane . . . 21

3.2 Cooperativity . . . 22

3.3 The effect of charged proteins on the transition in membranes: The Ising model . . . 23

4 Results **25**

4.1 Peakpositioning in deuterated water . . . 25

4.2 Meltingprofiles and heatcapacityprofiles of DMPG with and without cytochrome c . . . 26

5 Discussion and conclusion **30**

5.1 Context and outlook . . . 30

1 Introduction

1.1 Motivation

The immediate aim of this thesis is to examine how the peripheral protein cytochrome c affects the melting transition of a charged lipid membrane consisting of dimyristoylphosphatidylglycerol (DMPG).

In order to appreciate the essence of this thesis it is an advantage to comprehend the basic concepts of the biomembrane.

Furthermore to understand why it is interesting I will place the aspects of this thesis in the context of a *nerve pulse-theory* it relates to.

Consequently I will briefly describe the biomembrane[1] , its components and other features necessary to appreciate the theory it supports.

The theory suggests that the nerve pulses are *soundwaves travelling through the membrane* and not *electrical discharges travelling along the membrane* as the established theory states.
The evidence delivered by this thesis is for obvious reasons restricted to a few aspects of the whole story.

1.2 The cell

Cells can be considered the basic compartments of life. Their shape, size, composition differ from cell to cell depending on its environment and the role it is set to play.
The main division is that made between eukaryotic and procaryotic cells.
Eucaryotic cells are comparably big, they have the DNA separated from the organelles by a nucleus and they play distinct roles in multicellular organisms (humans etc.).
Procaryotic cells are smaller, single-celled organisms that live independent lives (bacteria etc.).

1.3 Biomembranes

The biomembrane is what separates a cell interior from the surrounding environment. Without a physical boundary it is not possible to obtain life since diffusion over time will make *the living* inseparable from *the surroundings*.

[1] I will denote the complex membranes found in real life: *biological membranes* or *biomembranes* whereas I will denote artificial monolipidmembranes: *lipid membranes* or *membranes*

The biomembrane is approximately 5 nm thick[1] and consists of various *lipids* and *proteins*. The proteins are embedded in a lipid matrix. They may span all across the membrane or bind to one side According to the *fluid mosaic model* the proteins are distributed randomly and both the lipids and the proteins are able to move around freely as buoys in the sea (see figure 1). [2]
Besides being containers for organelles the membranes themselves play many crucial roles and it is hard to overestimate their importance.

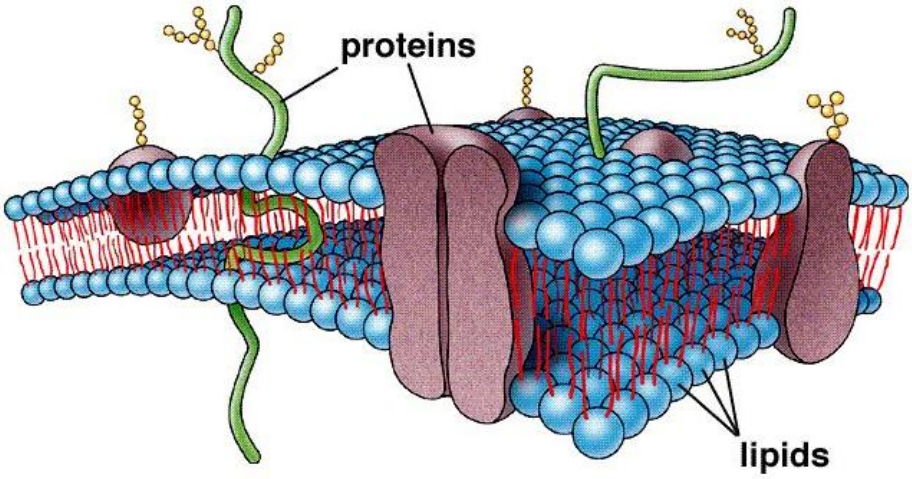

Figure 1: The fluid mosaic model of a biomembrane
Biomembranes are not just barriers - they play active roles in many biological phenomenons

The biomembrane is permeable to water and small uncharged molecules such as oxygen. Larger molecules and ions cannot freely diffuse cross the bilayer. This leads to concentration gradients across the membrane and osmotic stress that can be exploited favorably by the cell.
The biomembrane can consist of up to 500 different lipids that each have different chemical, physical and thermodynamical properties. [1]

1.3.1 The lipids

A lipid consists of a *headgroup* with one or more hydrocarbon *tails* attached (see figure 2) The headgroups differ from each other in size, charge and polarity. The headgroups are hydrophilic.
A lipidtail is a hydrocarbon chain. The lipidtails differ from each other in length - i.e. number of carbonatoms and their degree of *saturation*. A lipid is said to be unsaturated if it contains one or more doublebonds between the carbonatoms.

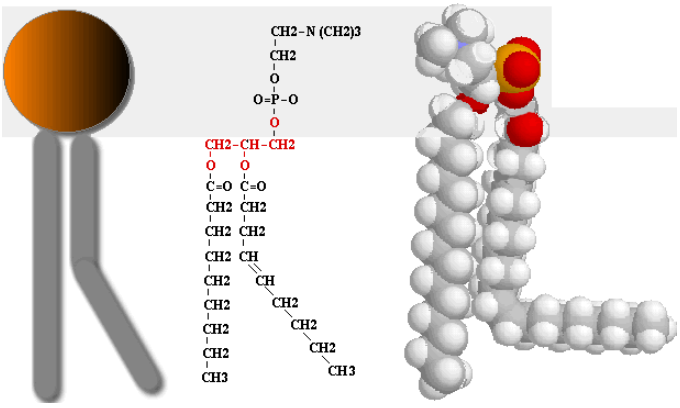

Figure 2: Three schematic drawings of an unsaturated lipid. The unsaturated bond is the crooked doublebond in the right tail

As opposed to the head, the lipidtail is hydrophobic The hydrophobic repulsion arises because the presence of lipidtails amongst watermolecules decreases the overall entropy by limiting the watermolecules access to the *phase space*[2].
Thus the chemical properties of the head and the tail are very different. This makes lipids a very poor soluble in water (but highly soluble in organic solubles (ether, chloroform, etc.)). The lipid of main interest for this thesis is dimyristoylphosphatidylglycerol (from here on referred to as DMPG). It is saturated and has two tails with 14 carbonatoms in each. Moreover it is a positively charged lipid which allows for electrostatic binding of peripheral proteins (see section 1.3.2).
When lipids are brought in contact with water they spontaneous arrange in groups where the tail-to-water surface can be minimized. The resulting structures are micelles, bilayers and series of parallel roles[3][3] (see figure 3).
The bilayer is biologically speaking the most interesting since it is this structure that

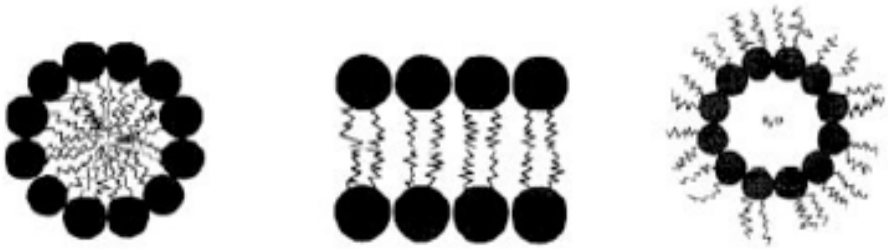

Figure 3: Micelle, bilayer and inverse hexagonal series of parallel roles
The different structures formed by lipids exposed to water

[2]The allowed configurations of the lipidtail in the presence of watermolecules
[3]also referred to as *inverse hexagonal phase structures*

makes up the biomembrane.
In a bilayer the tails in the two layers point toward each other. The headgroups point inwards to the cell center and outwards to the surroundings respectively (see figure 3). This is energetically a favorably structure and thus corresponds to a maximum of entropy.

1.3.2 Proteins

Proteins are large organic compounds made of amino acids. They play many crucial roles in all living organisms. Proteins may be membranebound or function as organelles in the cell (enzymes, etc).
The composition of the aminoacids determines a unique structure for the protein. The complex structure of proteins masks the correlation between protein structure and function. This may have a tendency to imposes opaque teleological explanations. In (figure 4) is a picture of a protein (right) and a schematic drawing of a causal correlation involving numerous proteins. This type of drawing is typical for textbooks in biology and biochemistry. It leaves out the all other properties of the biomembrane than *being a barrier*. Thermodynamical variables are not included either.

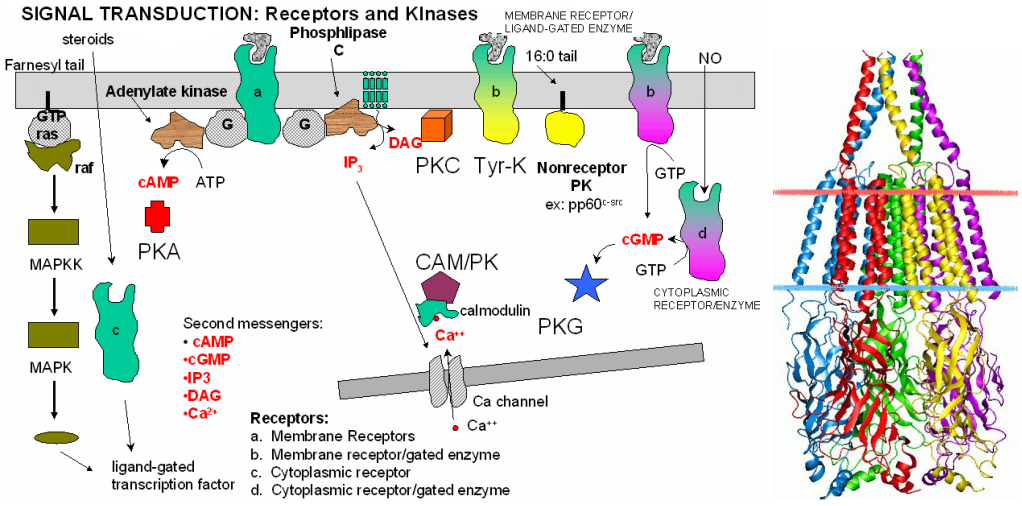

Figure 4: Left: An example of a opaque schematic correlation. Right: cytoplasmic receptor enzyme

A lot of biochemistry is based on the functions of proteins.
Thermodynamics does not play a role

Membranebound proteins are either embedded in the lipidmatrix or bound to one side. The latter are called peripheralproteins and their binding is mainly of electrostatic nature. When proteins bind to the biomembrane the shape and hence the function of the protein may change. [4] Another aspect of the binding is the less exploited fact that functions of

the membrane also changes due to altered thermodynamical properties.[5]
Cytochrome c is a peripheral protein. At low lipid/protein ratios it binds electrostaticly to charged lipids in the biomembrane but at higher ratios partial penetration of cytochrome c into the membrane occurs. [6]

1.3.3 The melting of the biomembrane

In a fully saturated lipidtail each $C-C$ bond has 3 possible configurations. The regular *trans-configuration* corresponds to the minimum energy. The two additional configurations are called *gauche-configurations*. A gauche-configuration results from a 120° rotation around the $C-C$ bond (see figure 5). Gauche-configurations have a higher internal energy and are therefore less accessible.
When the temperature is low the lipidtails will be at the minimum energy - all-trans-

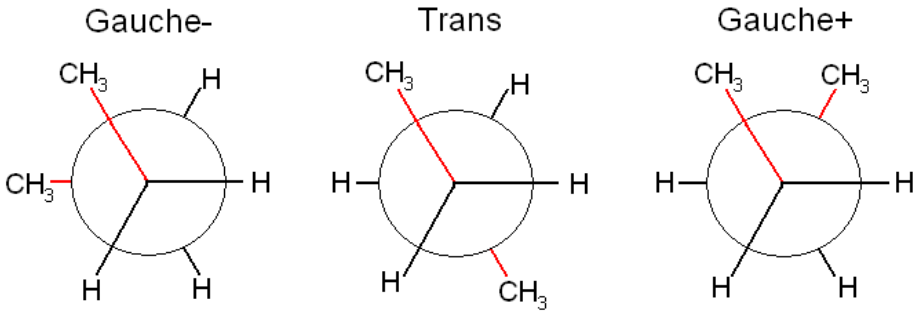

Figure 5: The three possible configurations for each saturated $C-C$ bond
The trans-configuration is the most probable at low temperatures. At increasing temperatures the rate of gauche-configurations raises

configuration. But when the temperature raises the trans-gauche energy gap becomes negligible. Hence the gauche-configuration becomes more probable due to its higher degeneracy. Finally at high temperatures the ratio of gauche-configuration approaches 2/3. [1]
4 phases of the bilayer are defined: [1]

- L_c - crystalline in three dimensions (all trans)
- L_b - gel phase (all trans)
- P_b' - ripple phase (trans/gauche)
- L_a - fluid phase (trans/gauche)

The temperatures at which the transitions between the phases take place are well defined. They depend on lipid composition, embedded proteins and various thermodynamical properties. Embedded proteins may broaden and shift the temperature at which the transition

takes place. I wil The shift from *gel* to *ripple* phase is known as the *pretransition* and the

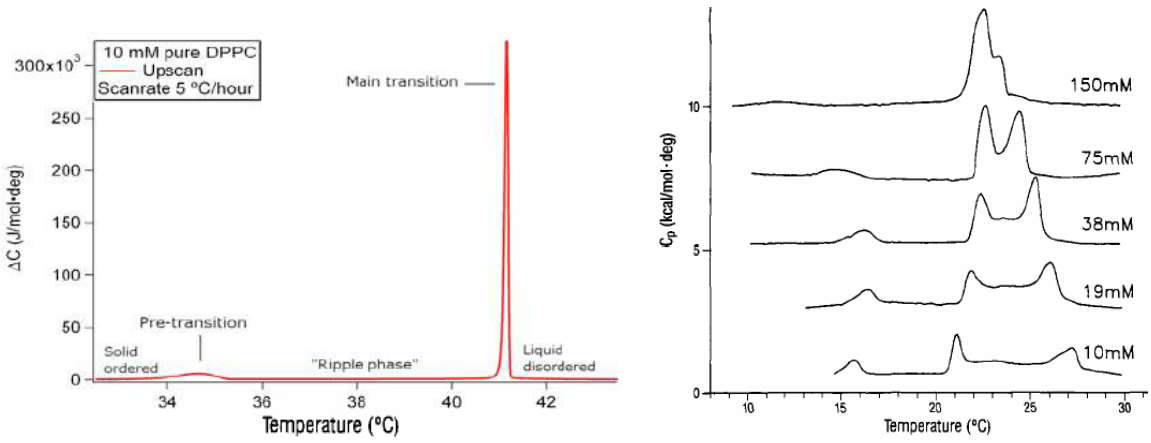

Figure 6: Left: The phase transition of DPPC (from [1]). Right: The phase transition with various dispersions of DMPG in a buffer(from [5]).

shift from *ripple* to *fluid* phase is the *maintransition* (see figure 6 left).
The maintransition is the biggest transition and forthcoming I will address the maintransition when I refer to the transition with no further descriptions.
The transition changes various properties of the membrane. A lipid with gauche-configurations is shorter and broader. Consequently the melted membrane is thinner but wider.

The meltingprofile of DMPG looks rather obscure (see figure 6 right). The structures formed by hydrated DMPG[4] depends on various thermodynamical variables. At low concentrations and temperature DMPG forms other structures than the membrane bilayer and consequently displays a different meltingprofile.
The meltingprofile displays a *shoulder* in the maintransition even for very high lipid concentrations (see figure 6 right).
For dipalmitoylphosphatidylcholine (DPPC) the meltingprofile is independent of concentration in the range of concentrations used for the experiments for this thesis ($c \sim [10mM - 100mM]$). The transition of pure DPPC is very sharp. It is only about $0,5°C$ wide.
Some proteins bind more favorably to specific structures. Therefore the addition of proteins can alter the preferred structure for a lipidspecies at a given concentration. [5]

During the transition the enthalpy rises hence the heat capacity peaks during the transition (Heat capacity is defined as ΔEnergy/ΔTemperature).
Furthermore calculations and experimental evidence show that compressibility and relaxation times also reach maximum in the transition range. [7]

[4]DMPG dissolved in water

The non-linear behavior of the compressibility as a function of the intensive thermodynamical variables is very important (temperature, pressure etc.). I will return to that in section 1.6.

1.4 Cooperativity and domain formation

In the fluid mosaic model from 1972 [2] (see section 1.3) lipids and proteins can diffuse freely but interaction between molecules is not considered [8] hence the lipid distribution is expected to be random.
In the mattress model from 1984 [9] it is suggested that the hydrophobic interactions play a role in the distribution of the lipids. This leads to domain formation of lipids and proteins with equal length[5].

The melting of a lipid induces the melting of nearby lipids thus the transition of monolipid membranes are confined to a much more narrow temperature range than calculations predict assuming independent melting of lipids. [1] When more than one lipid is present in the membrane the staggered meltingpoints reduce the effect of the induction. Furthermore it is energetically favorable for the melted lipids to have other melted lipids as neighbors because they have equal length. Subsequently domains can form which lead to coexistence of gel and fluid phases. [8]

Monte Carlo simulations show how cooperativity between lipids stimulates groupmelting. [10]
These simulations are computermodels that can predict domainformation in the transition of lipidmixtures from simple assumptions about cooperativity. Furthermore proteins and their bindingproperties can be included in the model (see figure 7 The transition is in most cells found to lie in the vicinity of the temperature of the surrounding environment. Bacteria grown at various temperatures compose their membranes so that their meltingpoint is near the temperature at which it is grown.
It seems to be essential for the cell to have the phase transition within reach (i.e. be able to *enter* the transition by means of small thermodynamical perturbations. [11]

1.5 The role of anaesthetics

Anaesthetics are drugs that bloc sensations and perceptions of pain. It is very useful in surgery as it enables sergeants to perform long and complicated operations without having to deal with screaming patients.
Though the effects of anaesthetics have been known for ages the actions that lead to anaesthesia are still a mystery.

[5] Two neighboring lipids of different length results in exposure of hydrophobic sites to the water.

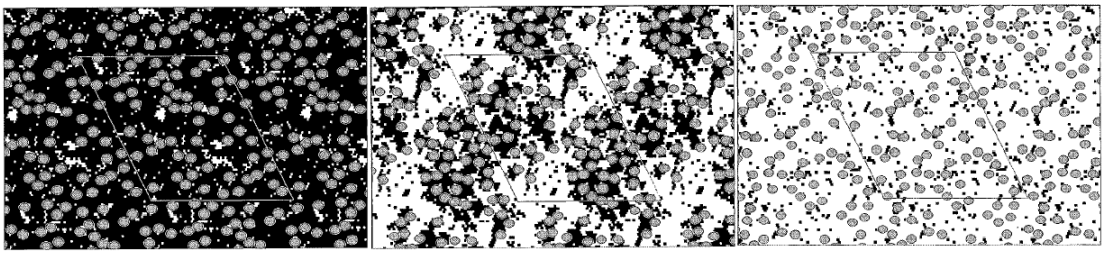

Figure 7: Left: below transition ($35.15°C$). Center: in transition($39.40°C$). Right: above transition($45.15°C$). The fraction of melted lipids are 0.09, 0.52 and 0.91 respectively. Monte-Carlo simulation for a membrane containing peripheral proteins. The black dots are gel-lipids, the white dots are fluid lipids and the circles are proteins. The distribution of proteins is random below and above the transition but not in the transitionphase where fluid and gel domains coexists. The figure is from [10].

It is widely believed that the target of anaesthesia is some proteins in the biomembrane responsible for iontransport across the membrane. There is clear evidence that some proteins are affected by anaesthetics but a satisfactory explanation is deficient. The established theory lacks specificity. [12]
Furthermore the disparity between different anaesthetic compounds is salient. The physical and chemical properties of anaesthetics vary greatly (some noble gases even qualify as anaesthetics). Furthermore the same anaesthetics affect most animals though the membraneproteins vary from species to species.
This suggests that anaesthesia is caused by something other than the immediate interaction (i.e. binding) of anaesthetics to the proteins of the membrane . [11]
More than 100 years ago a striking correlation between anaesthetic compounds was found. *The Meyer-Overton relation.* It relates the efficiency of an anaesthetic compound [6] to its partitioncoefficient between oil and water (see figure 8).
This is interesting because it means that the efficiency of an anaesthetic is based on how well it dissolves in the membrane. The Meyer-Overton correlation therefore strongly indicates that the immediate target of anaesthetics is the membrane.
If the target of anaesthetics is the membrane a question still remains; *How does anaesthetics in the membrane cause anaesthesia?*
It has been shown that anaesthetics alter the transition in membranes to a lower temperature. In biological membranes this means that the transition temperature is shifted *away* from that of the surrounding environment.

[6] The efficiency of an anaesthetic is measured in *Effective anaesthetic concentration* [ED_{50}] and was by Overton measured as the amount of a given anaesthetic needed to make tadpoles stop swimming.

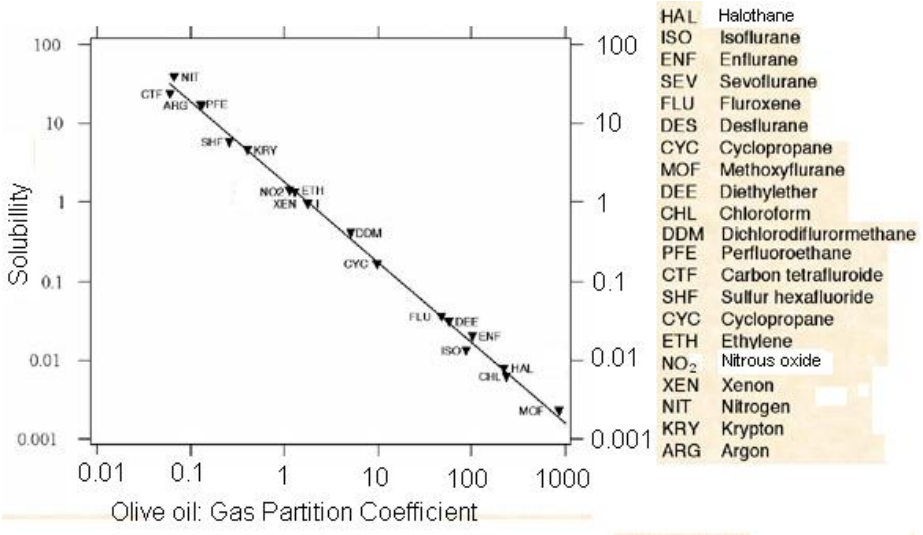

Figure 8: The Meyer-Overton correlation

1.6 Neurons and nerve pulses

In the *Hodgkin and Huxley* model on nerve pulses the ions run through specific ion-channel proteins. The proteins function as conductors and the membrane function as a capacitor. [13]
This description is purely electrical. It does not contain any thermodynamical variables. Furthermore a pressing problem with the model is that it falsely predicts a heat production in the nerve. Experiments suggest that the process that drives the nervepulse is reversible.

If a membrane is slightly above the transition temperature it will lower its elastic modulus when compressed. It is showed in [14] and [15] that this allows for the possibility stable propagating *solitons*.
that this allows for the possibility stable propagating *solitons*.
Heat capacity, volume and area compressibility and relaxation times reach maximum and the compressibility of the membrane is nonlinear in the transition. There are many indications in favor of the soliton model of nerve propagation. The nonlinear behavior compressibilities as functions of temperature and pressure in the transition domain accompanies the possibility of soliton propagation.
Furthermore is is shown [7] that the velocity of a soliton is approximately that of a nervesignal in a myelinated axonmembrane $v_{nerve} \approx 100m/s$.

2 Materials and methods

2.1 FTIR-spectroscopy

A molecule can absorb energy from infrared light if the frequency of the light corresponds to a vibrational frequency within the molecule. This phenomena is exploited in FTIR-spectroscopy (see figure 9).
An infrared lightpulse[7] is generated and shun through a *beamsplitter*[8]. The lightpulse is split and a time delay is induced in one of the pulses by the moving mirror before the lightpulses are reunited. The united pulse is subsequently shun through the sample and the transmitted signal contains data that can be translated into an *absorbtionspectrum* by means of *fourier transformation*. [16]
The transmitted signal is a rapidly decaying composite of frequencies. It is called *the free induction decay* and is a temporal coherence measurement of the resultant lightpulse. The fourier transformation changes the phase space from time-space to frequency-space.
This technique is very fast compared to the regular infrared spectroscopy. Here one frequency is shunned through the sample at a time and the absorption is measured.

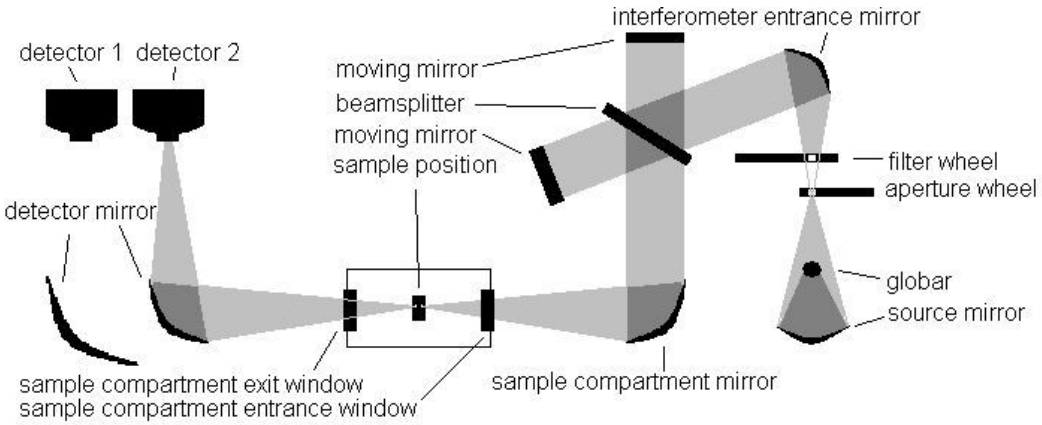

Figure 9: Beampath through the FTIR-spectrometer
The moving Michelson-Morley mirror and the beamsplitter is the heart of the FTIR-spectrometer.

I started out doing experiments with a lens that did not require cooling (Lens setting: position 1. on the FTIR). Although the waves looked good (no figure) the errorranges turned out to be too big ($0,3 \sim 15\%$). The total shift in wavelenght is only about $2cm^{-1}$
For all experiments in this thesis a lens that required cooling was used (Lens setting: position 2. on the FTIR). The apparatus was cooled using liquid nitrogen. The apparatus was

[7] I.e. a lightpulse that contains all the frequencies in the infrared spectrum
[8] Or a silvered-half mirror that transmits half of the light and reflects the other half.

Table 1: Charactaristic wavelengths of C-H bonds [17]. The bonds present in saturated lipids are *methylene*-bonds

Bond	**Bond type**	**Wavenumber [cm^{-1}]**
alkyl C-H	methyl	1260, 2870, 2960
alkyl C-H	methylene	1470, 2850, 2925
alkyl C-H	methine	2890
vinyl C-H	$C = CH_2$	900, 2975, 3080
vinyl C-H	$C = CH$	3020
vinyl C-H	monosubstituted alkenes	900, 990
vinyl C-H	cis-disubstituted alkenes	670, 700
vinyl C-H	trans-disubstituted alkenes	965
vinyl C-H	trisubstituted alkenes	800-840
aromatic C-H	benzene/sub. benzene	3070
aromatic C-H	monosubstituted benzene	690-750
aromatic C-H	ortho-disub. benzene	750
aromatic C-H	meta-disub. benzene	750-800, 860-900
aromatic C-H	para-disub. benzene	800-860
alkynes C-H	para-disub. benzene	3300
aldehydes C-H	para-disub. benzene	2720,2820

Table of charactaristic bonds [18]

set to 32 scans for each measurement and the scanrate was 20° per hour.

The $C - C$ bonds in the lipidtails show as two small peaks at $2920cm^{-1}$ and $2851cm^{-1}$ (see figure 10 and 11). The former peak results from the *symmetrical* vibrations and the latter from *asymmetrical* vibrations.
The two peaks are equally well defined but the symmetrical peak lies in the vicinity of the waterband (and partly overlaps it. See figure 10).
Hence all measurements in this thesis is performed on the asymmetrical peak[9].
The shift from trans- to gauche-configuration in the C-C bonds of the lipidtail also shifts the peak-position since the gauche-configuration corresponds to a slightly higher internal energy.

2.1.1 Peakpositioning and generating a meltingprofile

With each datafile corresponding to a temperature the peakposition as a function of temperature was obtained from the datafiles. The polynomial fits were done in IGOR by a

[9]When I refer to the C-C peak with no further specification it will be understood that the reference is for the asymmetrical peak.

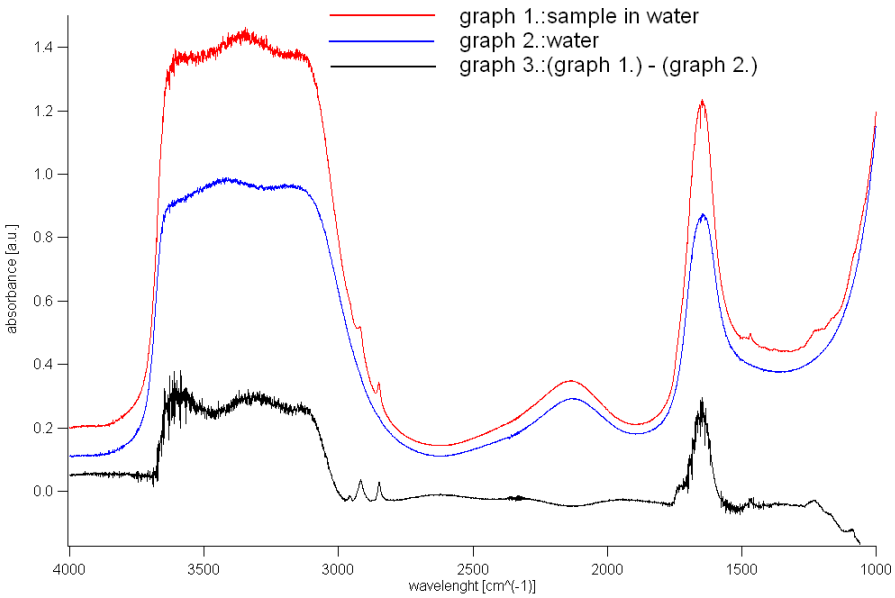

Figure 10: Isolation of DPPC-peak
Absorbance of: **1.** DPPC at 20 C., **2.** water at 20 C., **3.** (graph **1.**) -(graph **2.**)

program friendly provided by M. Fidorra.
The pretransition was only detectable in monolipidmembranes.
The change in wavelength corresponded to a change in internal energy. By differentiating with respect to temperature the heat capacity was obtained. In the vicinity of the main-transition where the slope was steep the heat capacity peaked.

The data from the FTIR-spectrometer was read by OPUS and via a program (written by M. Fidorra) converted to *txt*-files. The *txt*-files contained data in two rows each. Wavenumber $[cm^(-1)]$ and absorption $[a.u.]$. One file corresponded to one scan and since each experiment was made with scans every $1/2°C$ an experiment over a temperatureinterval of $60°C$ contained 120 files.
In IGOR each file was baselinecorrected (see figure 11 left). This was necessary due to the overlap of the waterband. Subsequently a 3^{rd} order polynomial was fitted to the data of each file in the vicinity of the peak (see figure 11 right)[10].)
A plot of the peakpositions from each file as a function of temperature (temperature,peakposition) provided the *meltingprofile* of a specific biomembrane (see figure12). It show how the wavelength of the light absorbed by the sample changed when the temperature of the sample changed.
The meltingprofile was differentiated with respect to temperature to obtain the heatca-

[10]Differentiation of the fit locates the exact position of the peak.

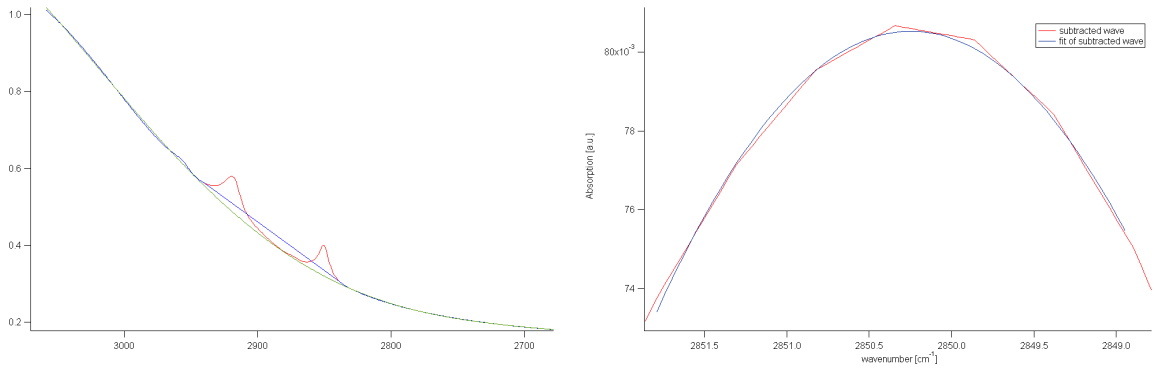

Figure 11: Left: subtraction of baseline. Right: fit to wave (see appendix figure 23) for enlargements

Correction of baseline and polynomial fit to peak

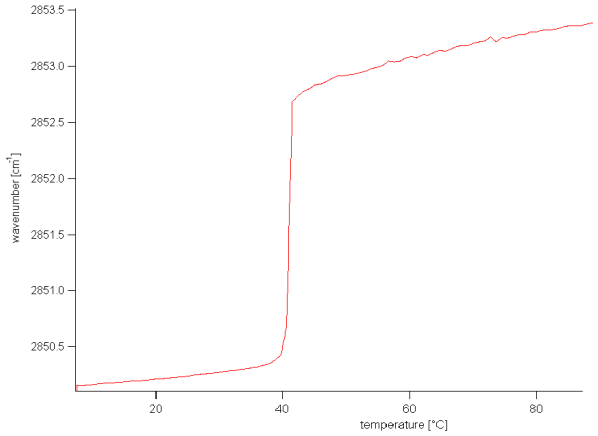

Figure 12: Meltingprofile: peakposition as a function of temperature
The meltingprofile display the peakposition as a function of temperature and shows the transitions of the biomembrane. The transition is very sharp for pure DPPC

pacity profile[11].
In order to obtain a differentiable graph for the melting profile each point p_i was fitted to a third order polynomial together with a number n of the prior and subsequent points (i.e. a polynomial fit of the points p_{i-n} to p_{i+n}).
If the transition was steep n had to be very small (i.e. $n = 1$ or $n = 2$) in order to get a reasonable heatcapacity profile. When n was small the noise from small variations also became more visible in the heatcapacity profile (see figure 13). Hence a proper value n was found for each experiment.
Both the determination of the peakposion and the differentiation was done with a program

[11]Energy differentiated with respect to temperature is heat capacity: $\frac{\delta E}{\delta T} = c_p$.

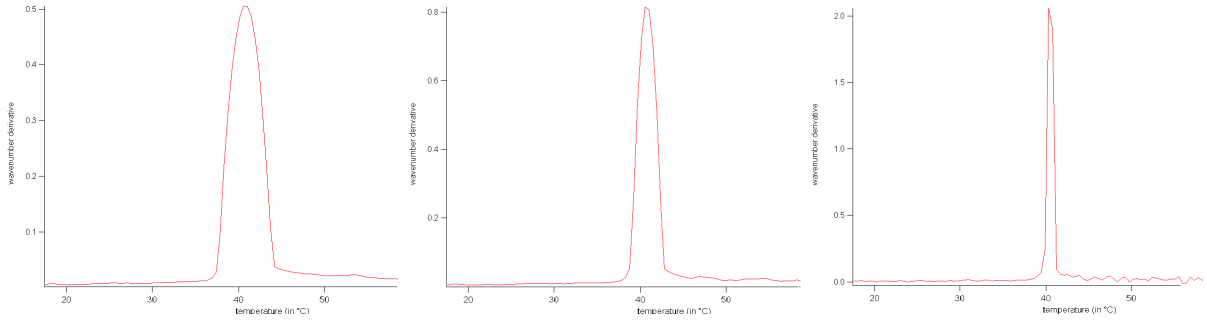

Figure 13: Left: $n = 7$. Middle: $n = 4$. Right: $n = 1$
Heatcapacityprofiles derived from various n-values

provided by M. Fidorra.

2.2 Sample preparation

The cellmembranes used in the experiments were all synthetic - that is - made from isolated, identical lipids in powder form. The lipids were from Avanti Polar Lipids (Alabaster/AL, USA) and used without further purification.

The lipidpowder was dissolved in chloroform in a concentration of about $10\frac{mg}{ml}$.
In experiments with more than one lipid the desired amount of lipids in aliquots were mixed and whirled.
The amounts of lipidpowder needed was calculated into mole fraction from the known correlations

$$c = \frac{n}{V}$$

and

$$n = \frac{m}{M}$$

Where c is concentration, n is number of moles, V is volume m is mass, M is molarity.

The chloroform was evaporated. The lipids were put in a desiccator for two hours to extract the last chloroform residues. Subsequently the lipids were hydrated at a temperature above the meltingtemperature of the relevant lipids (if more than one lipidspecies was mixed the temperature was set above the highest of the meltingtemperatures).
The same procedure was followed when adding oil-dissolvable proteins. The samples were stored at approximately $5°C$ and experiments were performed up to 14 days after date of preparation.

Due to risk of bacteria growth in the sample they were thrown out after this point.

2.2.1 The chamber

The chamber consisted of two CaF_2-crystals separated by two pieces of $12\mu m$ thick *spacers*(see figure 2.2.1 above). The rubber rings prevented the crystals from breaking when the top was put on.
The lipidmixture was pipetted onto the lower CaF_2-crystal before the upper CaF_2-crystal was put on top (see figure 2.2.1 below). Approximately $100\mu l$ of sample was used for the measurements.
It was important that no air bubbles were trapped between the crystals. This would disturb the measurements when the sample was heated and the air bubbles expanded.
The chamber was fabricated to fit a holder in the FTIR-spectrometer. This allowed for

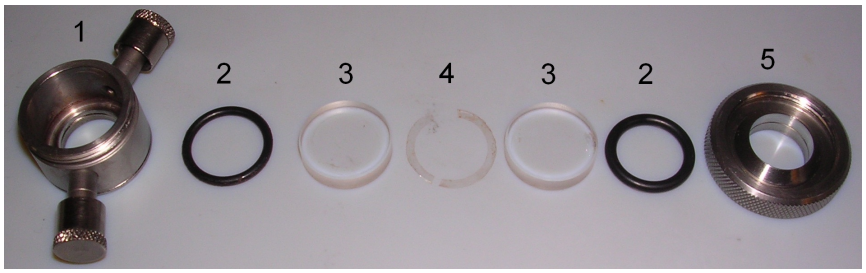

Above: The parts of the chamber: **1:**chamber, **2:**rubber rings, **3:**CaF_2-crystals, **4:**$12\mu m$ spacer, **5:** lit. **Below:**The sample was pipetted onto the CaF_2-crystal

Figure 14: The chamber used for measurements

rising and lowering the chamber in the FTIR-spectrometer without letting air into chamber.
Furthermore the holder was coupled to a thermocouple that controlled the temperature of the chamber.

2.3 Samples in deuterated water

The lit was kept on the deuterated water as much as possible to prevent hydrogen from the air humidity from being exchanged with the deuterium. The samples were prepared in the same way as for the regular experiments but buffer was not used and experiments were performed no longer than 10 minutes after sample preparation.
The experiments performed with deuterated water were prepared in the same way as samples with regular water or buffer.

2.4 Estimate of errors

As in all other experimental work errors errors are present.
In preparation of the samples the lipids and the proteins were measured on a scale. The scale had a precision of $10^{-4}g \sim 1\%$ of the lipids and $\sim 0,5-2\%$ of the proteins for a sample.
The binding of cytochrome c to the membrane is difficult to estimate for different protein/lipid ratios. All proteins in the samples are expected to bind to the membrane.
Furthermore the pipettes had an estimated errorrange of 1% The peakpositioning was very accurate (see figure 11). The deviation was taken to be $\leq 0,1cm^{-1}$. But since the overall shift in wavenumber is only about $2cm^{-1}$ the deviations is worth considering. It corresponds to noise of about 5% of the *wavenumber-axis* in the meltingprofiles.

2.4.1 Temperature calibration

To calibrate the FTIR-temperature controller a wire connected to a thermocouple was plugged into the sample holder. By doing a temperature scan via the OPUS macro program the temperature on the FTIR-temperature controller and on the thermocouple was read simultaneously and compared. (see figure 15)
The temperature calibration scan ran from $15-75°C$. This was the range in which most experiments were performed[12] The calibration revealed a deviation nearly linear to the temperature increase (see figure 15). For small temperatures ($T \leq 30°C$) the chamber temperature lyes within $0,5°C$ of the temperature controller.
The calibrationdata can be described well by a straight line. Hence the temperaturescan is linear in time but the increase per hour is different then that of the temperature controller. The coefficient for the linear datafit is $a = 0,893$ which implies that the scanrate is:

$$scanrate = 0,893 \cdot 20\frac{°C}{hour} = 17,86\frac{°C}{hour} \tag{1}$$

The lowering of the scanrate arises because heat is lost in the pipes leading temperature controlled liquid from the controller to the sampleholder. This effect is not expected to

[12] except for the experiment on DMPG and cytochrome c $(8-50°C)$

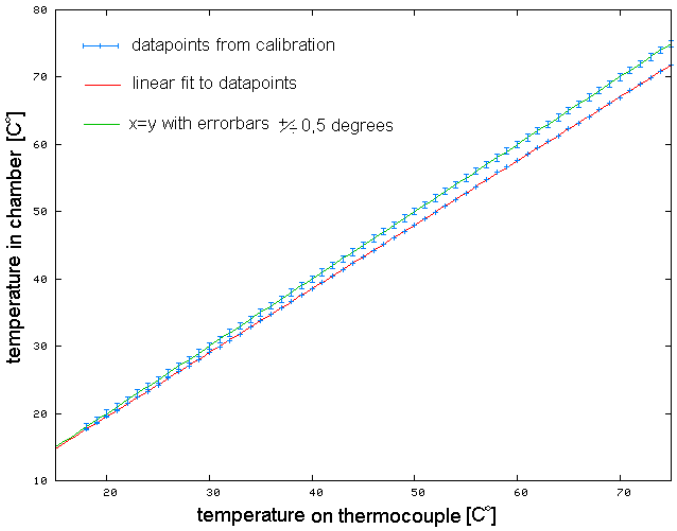

Figure 15: The temperature in the chamber rises slower than that of the temperature controller

The temperature calibration with a thermocouple

be linear with increased temperature but rather exponential since the diffusion of heat is proportional to the the temperaturegradient between the laboratory and the pipes. Nevertheless the linear approximation is very good in the range from $15 - 75°C$(see figure 15). The linear fit does not intersect orego hence the calibration could not be done merely by dividing the *temperature-axis* by a. Instead the intersection of the two graphs in (figure 15) was taken as orego. The deviation from that point was subsequently divided by a. The point of intersection was $T = 12°C$[13].
All graphs in this thesis[14][15] is calibrated in this manner.
The calibrated graphs are expected to have an errorrange of no more than $0,5°C$.

The effect of this deviation of $0,5°C$ on the heatcapacityprofile is minimized by the fitting to nearby points. In the cases with $n = 7$ the fit is made over 15 points hence the errorrange is reduced significantly. When $n = 1$ the fit is limited to 3 points and furthermore three subsequent points are influenced by the same deviation (each point is included in its neighboring fits and its own). Hence low values of n gives rise to more noise.

[13]This is the temperature where the temperature on the thermocouple coincides with the temperature in the chamber according to the calibration fit.
[14]Exceptions are graphs borrowed from elsewhere.
[15]It includes previous graphs shown in this thesis

3 Theory

In this section I will deduce the meltingpoint of a biomembrane and how it is altered by the presence of proteins.
I will show the theoretical heatcapacityprofile is altered. This leads to various important properties of the cell (see section 1.6) [7] [11] [15]
The following calculations are thermodynamical and of a statistical nature. Thermodynamics is a branch of physics that is based on statistics. It describes a system by a number of interrelating variables. From these variables and with some simplifying assumptions a number of properties of the system can be deduced. Thermodynamics is not an exact science but it can be extremely accurate and useful for complex systems (like the biomembrane).

3.1 The meltingpoint of a homogeneous membrane

I assume that only two states are available for each lipid: gel (g) and fluid (l).
To find the meltingpoint T_m of a homogeneous membrane I express the probabilities of being in a given state i.
The calculations are from [1], [19] and [20].
From the canonical ensemble[16] I obtain:

$$P_i = \frac{e^{-H_i/k_b \cdot T}}{\sum_i e^{-H_i/k_b \cdot T}} \tag{2}$$

Since there are only two states the probability of being in state l is:

$$P_l = \frac{\Omega_l \cdot e^{-H_l/k_b \cdot T}}{\Omega_g \cdot e^{-H_g/k_b \cdot T} + \Omega_l \cdot e^{-H_l/k_b \cdot T}} \tag{3}$$

Where Ω_i is the degeneracy of state i.

$$P_l = \frac{\Omega_l/\Omega_g \cdot e^{-\Delta H/k_b \cdot T}}{1 + \Omega_l/\Omega_g \cdot e^{-\Delta H/k_b \cdot T}} \equiv \frac{K}{1+K} \tag{4}$$

And equivalently $P_g = \frac{1}{1+K}$

$$K = \frac{\Omega_l}{\Omega_g} \cdot e^{-H_l/k_b \cdot T} = e^{\left(\frac{\Delta H - T \cdot \Delta S}{k_b \cdot T}\right)} \tag{5}$$

With $\Delta S = k_b \cdot \ln(\Omega_l/\Omega_g)$

[16] Canonical ensemble: An isolated system with a number of subsystems. Each with constant volume and particles. Heat exchange is allowed between the subsystems.

K is the equilibrium constant. It defines the meltingpoint as: $K(T_m) = 1$
and so $P_l(T_m) = P_g(T_m) = 1/2$
From equation (5) I obtain an expression for T_m:

$$\ln(1) = \frac{\Delta H - T_m \cdot \Delta S}{k_b \cdot T_m} \tag{6}$$

$$T_m = \frac{\Delta H}{\Delta S} \tag{7}$$

It is shown [1] that both the change in entropy and enthalpy increases linearly with the number of carbon atoms in the lipidtail.
The enthalpy increases with a steeper slope. This leads to a higher meltingpoint for longer lipidtails.
We have defined a meltingpoint for a membrane consisting of a single lipidspecies from probabilities of configurations within the lipidtails.
In section 3.2 I will improve this model to include the cooperation of the lipids.

3.2 Cooperativity

The following calculations are from [10], [1], [19], [21], [22] and [20]:
In the transition $C_p = C_p(T_m)$ we have $\Delta G = 0$ and hence $T_m = \frac{\Delta H}{\Delta S}$
Derivation of the mean enthalpy with respect to temperature leads to the heat capacity of the system:

$$C_p = \left.\frac{\overline{\Delta H}}{dT}\right|_p = \frac{e^{-\Delta G/R \cdot T}}{\left(1 + e^{-\Delta G/R \cdot T}\right)^2} \cdot \frac{\Delta H^2}{R \cdot T^2} \tag{8}$$

From equation (8) the heatcapacity of a lipid is given as a function of temperature. The heatcapacity peaks in the transition of the lipidmembrane.
The transition obtained from equation (8) is much narrower than transitiongraphs obtained from experimental evidence. [1] [23]
This is caused by what is known as cooperativity (see also section 1.4).

We assume that the membrane is a plane matrix with a triangular lattice. (6 nearest neighbors). We can then derive an expression for the cooperativity.
The free energy of a lipid consists of internal energy G_i (i is either g or l) and a sum over the free energy from neighbor interactions: ϵ_{ij}
The membrane has n lipids and the energy of membrane is a sum over the energy of each lipid and its interactions:

$$G = n_g \cdot G_g + n_l \cdot G_l + n_{gg} \cdot \epsilon_{gg} - n_{ll} \cdot \epsilon_{ll} - n_{gl} \cdot \epsilon_{gl} \tag{9}$$

n_i is the number of lipids in the state i, n_{ij} is number of neighbor interactions in states i and j it can be written as:

$$G = n_g \cdot G_g + n_l \cdot (\Delta H - T \cdot \Delta S) - n_{gl} \cdot \omega_{gl} \tag{10}$$

We define $\Delta H \equiv (H_l + z \cdot \frac{\epsilon_{ll}}{2}) - (H_g + z \cdot \frac{\epsilon_{gg}}{2})$ and $\Delta S \equiv (S_l - S_g)$, with z being the number of nearest neighbors.
The excess free enthalpy (Gibbs free energy) of the membrane is then:

$$\Delta G = G - n \cdot G_g = n_l(\Delta H - T \cdot \Delta S) - n_{gl} \cdot \Delta\omega_{gl} \tag{11}$$

$\Delta\omega = \epsilon_{gl} - \frac{\epsilon_{gg} - \epsilon_{ll}}{2}$ defines the cooperativety of the lipids.
We have 3 parameters to determine: T_m, $\Delta\omega$ and ΔH
T_m can be determined as the peak of the heatcapacity profile. ΔH can be found as the integral over the heatcapacity profile. $\Delta\omega$ can be found by comparison between experimental evidence and the heatcapacity model.
When The cooperativity is small the transition is broad. The heat capacity is then reduces to equation (8):

$$C_p(T) = \frac{e^{-\Delta G/R \cdot T}}{\left(1 + e^{-\Delta G/R \cdot T}\right)^2} \cdot \frac{\Delta H^2}{R \cdot T^2} \tag{12}$$

High values of $\Delta\omega$ means that the lipids induce the melting of each other. This leads to very narrow transitions. In this case all vesicles of size N are in the same state:

$$C_p(T) = \frac{e^{-N \cdot \Delta G/R \cdot T}}{\left(1 + e^{-N \cdot \Delta G/R \cdot T}\right)^2} \cdot \frac{N \cdot \Delta H^2}{R \cdot T^2} \tag{13}$$

3.3 The effect of charged proteins on the transition in membranes: The Ising model

We now consider the *Ising model* for peripheral interactions of proteins with the membrane. The calculations are from [1], [21], [22] and [24] We assume that the the membrane can be in four states: *Fluid* (L), *Fluid and covered with proteins* (LP), *gel* (G) and *gel covered with proteins* (GP).
Furthermore we define equilibrium constants to describe the transitions between the different states:

$$\begin{array}{ccc} G + P & \overset{K_1}{\leftrightarrow} & L + P \\ K_2 \updownarrow & & \updownarrow K_3 \\ GP & \overset{K_4}{\leftrightarrow} & LP \end{array} \tag{14}$$

The rate constants must be path independent, hence:

$$K_1 \cdot K_3 = K_2 \cdot K_4 \tag{15}$$

But $K_1 \neq K_4$ since proteins on the membrane alters the heatcapacity of the membrane and therefore the meltingpoint. The free energy is a function of state and must also be independent of path, hence:

$$\Delta G_1 + \Delta G_3 = \Delta G_2 + \Delta G_4 \tag{16}$$

It follows that the bindingproperties of the gel membrane is different from the fluid membrane and hence the energies of their bindings are different: $\Delta G_2 \neq G_3$
The difference in the interaction energy of protein-gel membrane and protein-fluid membrane is:

$$\Delta G_p = \Delta G_4 - \Delta G_1 = \Delta G_3 - \Delta G_2 = \Delta H_p - T \cdot \Delta S_p \tag{17}$$

This can be rewritten as:

$$\Delta T_m = \frac{\Delta H + \Delta H_p}{\Delta S + \Delta S_p} - \frac{\Delta H}{\Delta S} \tag{18}$$

Experimental evidence can provide the excess enthalpy and shift in melting temperature (i.e. comparison of heatcapacity profiles).
For DMPG: $T_m = 297°K$ and $\Delta H = 6000 cal \cdot mol^{-1}$.

$$\Delta S = \frac{\Delta H}{T_m} = 20,2 cal \cdot mol^{-1} \cdot K^{-1} \tag{19}$$

When cytochrome c is added the meltingpoint is shifted $\Delta T_m = 5°K$ and the melting enthalpy is lowered: $\Delta H_p = -4300 cal/mol$. This results in a shift in entropy:

$$\Delta S_p = -\frac{\Delta T_m \cdot \Delta S + \Delta H_p}{\Delta T_m + \Delta H / \Delta S} = -13,9 cal \cdot mol^{-1} \cdot K^{-1} \tag{20}$$

This result indicates that binding of protein to the membrane in the is entropically favorable below the transition when the membrane is in the gel phase since this binding corresponds to the biggest entropyproduction.
See (figure 7).

4 Results

The following results are obtained from measuring with FTIR-spectrometer as described in section 2.

4.1 Peakpositioning in deuterated water

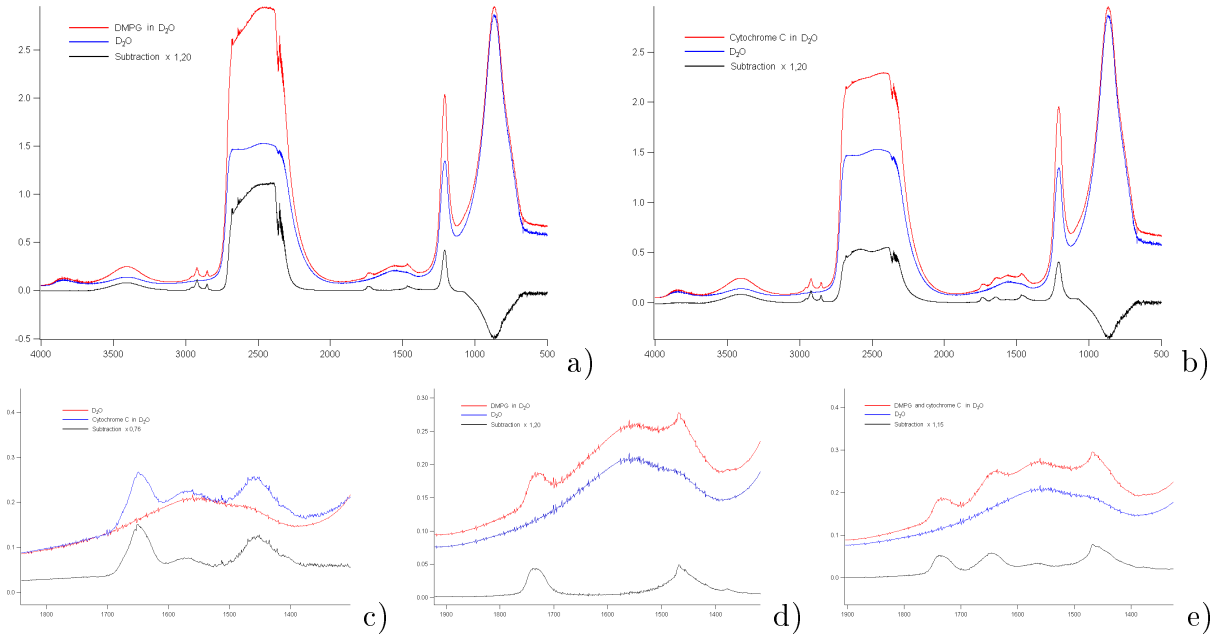

Figure 16: DMPG in deuterated water

The graphs in (figure 16) show characteristic peaks of DMPG and cytochrome c in deuterated water. The peaks in c), d) and e) at $1700 - 1600cm^{-1}$ and $1500 - 1400cm^{-1}$ are the *amide I* and *amide II* bands. In samples with regular water they are not visible due to noise from the waterbands in that region (see figure 10).
The spectra is a bit noisy. This may be due to a slight hydration of the water (deuterium is exchanged with hydrogen from the air humidity).
The noise made the peakpositioning difficult. The errorranges exceeded those from regular peakpositioning in normal water. Furthermore the deuterated water can not be exposed to air for very long without exchanging deuterium for hydrogen and hereby ruining the measurements. This makes deuterated water hard to work with.
All following peakpositioning is made from regular water.

4.2 Meltingprofiles and heatcapacityprofiles of DMPG with and without cytochrome c

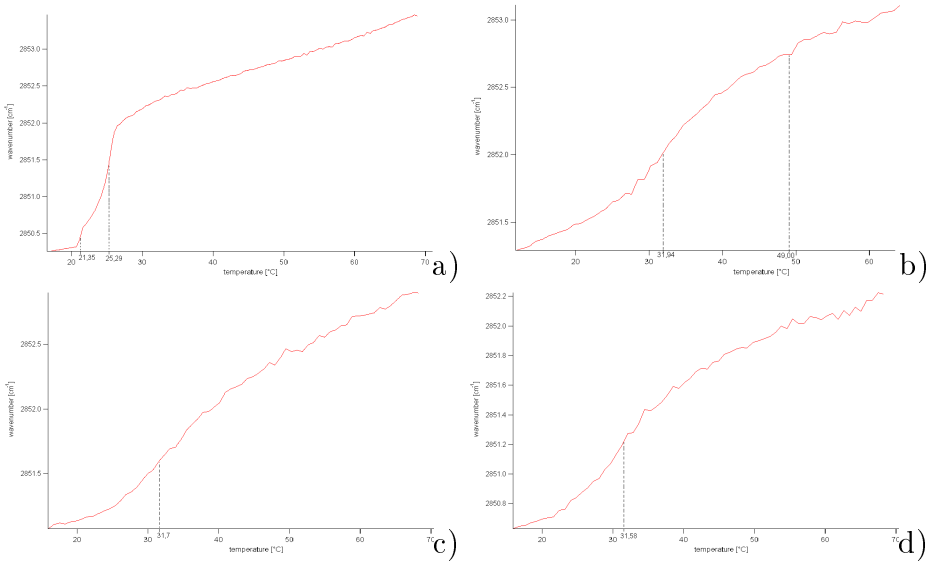

Figure 17: a) DMPG:cc - 1:0, b) DMPG:cc - 2:1, c) DMPG:cc - 1:1, d) DMPG:cc - 1:2
Meltingprofile of DMPG varying amounts of cytochrome c. Fraction by weight
$(2-1 \sim 2mg.$ DMPG to $1mg.$ cytochrome c)

In (figure 17) the meltingprofile is shown and in (figure 20) the heatcapacityprofile is shown. Both figures are for DMPG with varying amounts of cytochrome c. In (tabular 2) some numbers from the graphs are listed.
The peakpositioning of pure DMPG was difficult since the doublepeak in a narrow range made fitting to a 3^{rd} order polynomial over many points difficult. In (figure 18) differentiations of (figure 17 a) are shown with different values of n. The graph for $n = 1$ seems to be the one that determines the peaks with the highest precision. For discussion of n see (section 2)

From (figure 20) and (table 2) it is clear that cytochrome c shifts the two peaks of DMPG to a single peak at higher temperatures. There are indications that the temperatureshift does not vary significantly with proteinconcentration. In fact the peak of the heatcapacity is found to have the highest value for the lowest proteinconcentration (except for the pure DMPG which has the peak at lowest temperature).

The heatcapacityprofile is broadened and lowered significantly with the addition of cytochrome c. The hight of the peak is only about 20% of the peak of pure DMPG. This also seems to be independent of the amount of added cytochrome c (see table 2).

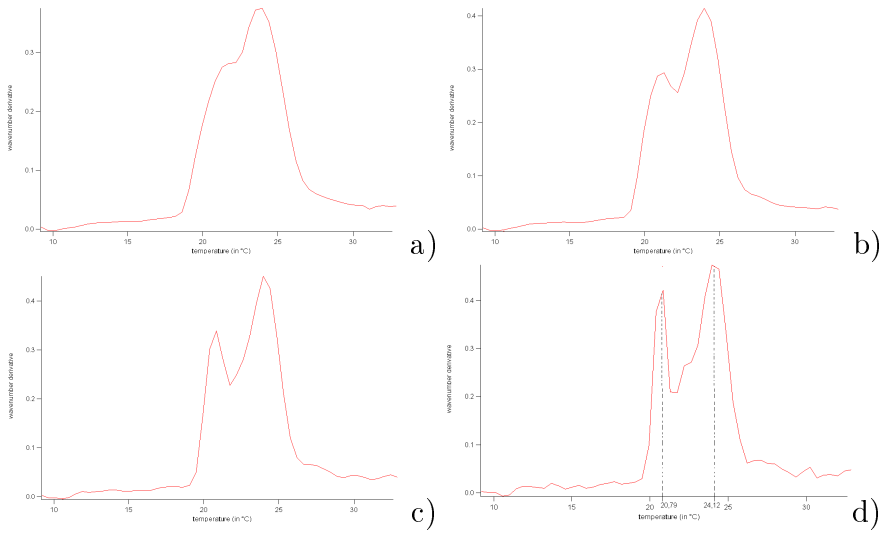

Figure 18: DMPG ($75mM$).
Different values of n for the heatcapacityprofile of pure DMPG. The complex form of the pure DMPG heatcapacityprofile requires a low value of n.

Figure 19: a)$n = 4$, b)$n = 3$, c)$n = 2$, d)$n = 1$.

The heatcapacityprofiles for DMPG with cytochrome c in (figure 20) are much more noisy than the profile of pure DMPG in the temperaturerange above the transition. There is a little peak in the range $49 - 55°C$ on all of the three graphs (figure 20 b,c,d). The peaks are small but they seem to be bigger than the mean deviation and therefore they can not be ignored.

Table 2: concentration of DMPG is in all cases $50mM$

protein/lipid fraction [weightfraction]	excess heatcapacity $[cm^{-1}C^{-1}]$	Peakposition $[°C]$
0/1	$\sim 0,40$	$21,35$ and $25,29$
1/2	$\sim 0,075$	$31,94$ (and $49,00$)
1/1	$\sim 0,075$	$31,70$ (and $54,88$)
2/1	$\sim 0,085$	$31,58$ (and $53,12$)

From the melting profiles and the heatcapacity profiles it is obvious that cytochrome c has an effect on the melting of the DMPG-membrane (see figure 21).
The transition of DMPG has two peaks for the concentration used at $20,5°C$ and and $24°C$ approximately. When cytochrome c is added the peaks are joined in a single peak at $20,5°C$ approximately. The single peak is broad and has a much lower heatcapacity profile (note the different scalings in the two graphs b) and d) in (figure 21))
In (figure 21) the heatcapacityprofiles of DMPG ($75mM$) with and without cytochrome c from another experiment is shown. The temperatureshift is from the doublepeak $20,79°$

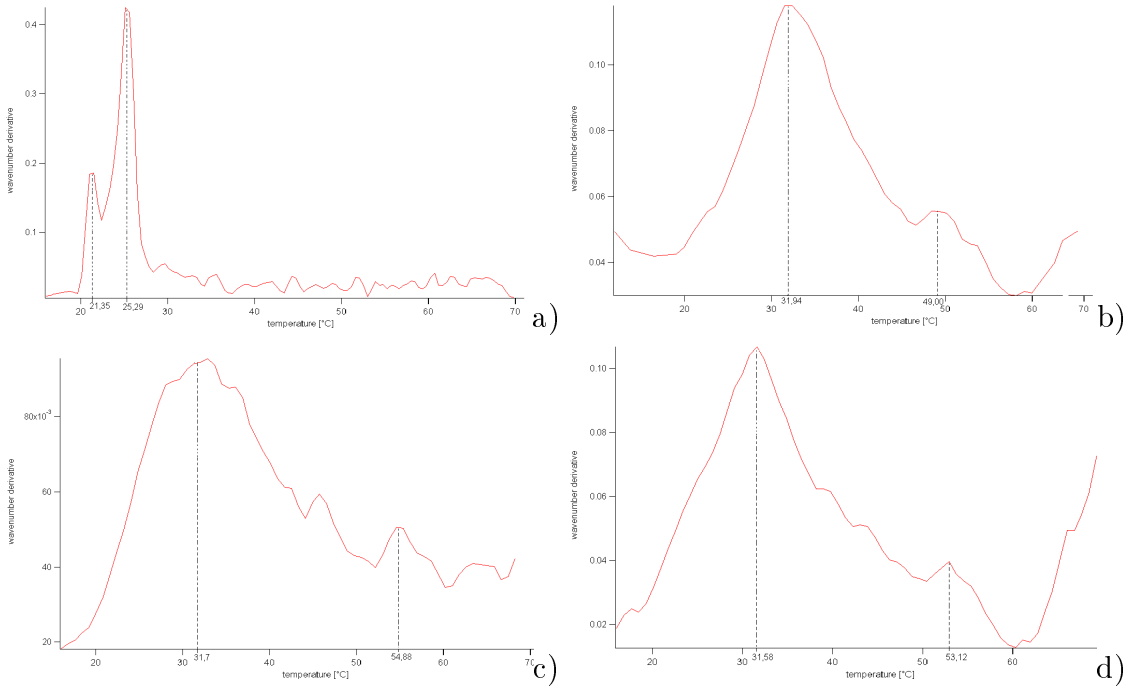

Figure 20: a) DMPG:cc - 1:0 (n=2), b) DMPG:cc - 2:1 (n=7), c) DMPG:cc - 1:1 (n=7), d) DMPG:cc - 1:2 (n=7)
Heatcapacityprofiles of DMPG with varying amounts of cytochrome c. Fraction by weight $(2-1 \sim 2mg.$ DMPG to $1mg.$ cyt. C)

and $24,12°$ to a single peak around 29° (see appendix figure 22 for this graph with different values of n).
All peaks of this experiment are found at temperatures approximately 1 degree below those of (figure 20) but the shifts are very close to those obtained in (figure 20). This could indicate that the calibration was not the same for the experiments.

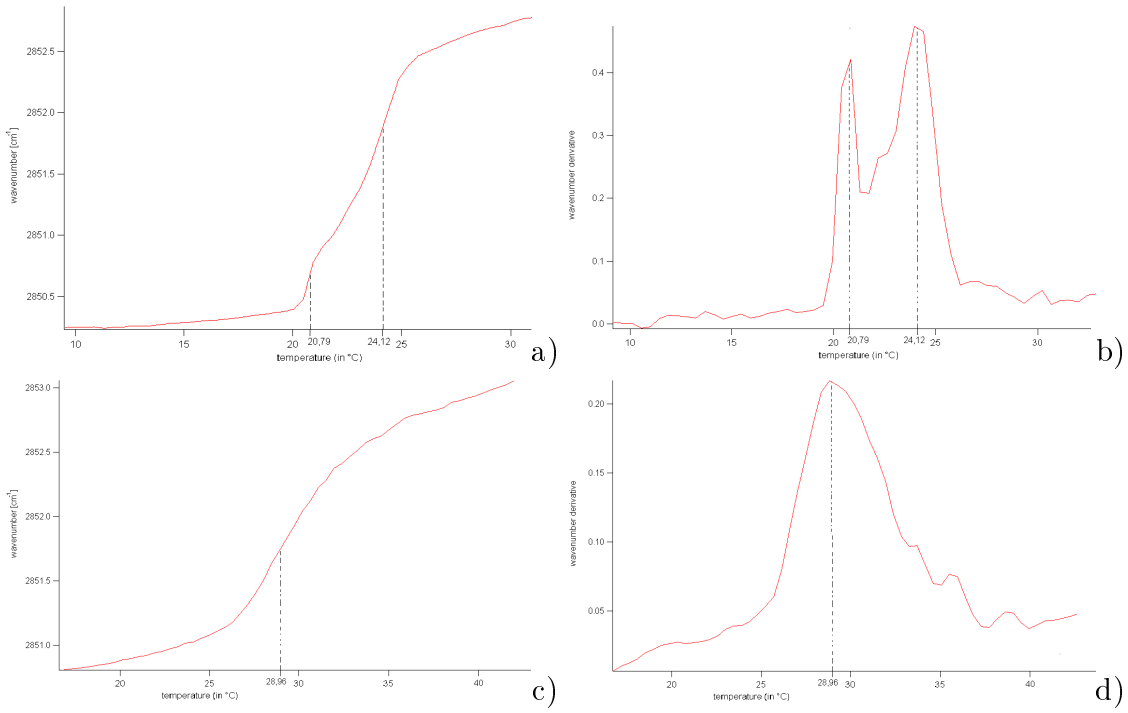

Figure 21: DMPG ($75mM$). a) and b): without cythochrome c. c) and d) with cytochrome c

5 Discussion and conclusion

The purpose of this thesis was to examine how the peripheral protein cytochrome c alters the melting transition of charged DMPG lipid membranes.
I found that cytochrome c shifts the meltingpoint of DMPG by approximately $6°C$. furthermore I found that the heatcapacityprofile was broadened and lowered by approximately 80%. This was true for protein/lipid-ratios from 1/2 to 2/1.
The heatcapacityprofiles were obtained by proper differentiation of the meltingprofiles which were generated from the shifts of the characteristic $C-C$ peaks observed with the FTIR-spectrometer. I used FTIR-spectroscopy for my measurements. This was very time consuming but the data contained more information then that of a calorimeter which can generate a heatcapacityprofile by a 10 minutes temperaturescan.
In all measurements with cytochrome c the two peaks of DMPG were reduced to a single peak (although a small unexplained peak was present in experiments with temperatureintervals up to $70°C$). The doublepeak is caused by an effect of cytochrome c that alters the preferred structure of DMPG (i.e. to the bilayer) at low temperatures for the lipidconcentrations used. This effect is presumably a energeticly more favorable binding to bilayers then to micelles etc.
It was expected that an increasing amount of cytochrome c would cause an increased effect (i.e. on heatcapacityprofile shift, hight and width). This was not the case.
This could be because the membrane was covered with protein already at 1/2-ratio and additional protein therefore only resulted in the same coverage of the membrane. Another option is that it is a result of poor mixing of DMPG and cytochrome c. If the sample was not mixed properly it could result in only partly binding.
The mixed sample was whirled for 5-10 minutes at approximately $50°C$ but maybe longer time was needed.

I tried experiments on deuterated water and located the *amide I* and *amide II* bands. The pakpositioning on these spectra was difficult due to noise from exchange of hydrogen from the air with the deuterium.

5.1 Context and outlook

The biological membrane of cells is a very complex matter. The investigation of the transition of such membranes is interesting because it causes various thermodynamical changes. These changes alters many properties of the membrane and what more is this transition and its resultant properties always lies *within reach* of most biological membranes.
Experiments suggest that anaesthesia is a result of a shift that sends in the transition *out of reach*. These results come from thermodynamical experiments and calculations and represent a quite different approach to biochemistry than the predominant one. The membrane is assigned a dominant role whereas it earlier merely was considered a barrier to hinder diffusion.

There are more than 500 different lipids and many different proteins present in an average biomembrane. I believe there are many properties and roles of the membrane there are yet to be understood.
I have merely showed some effects of a peripheral protein on a charged membrane but the properties that emerge from these and other changes in the transition of the biomembrane is a field where I think a lot of discoveries are yet to be made.

Litterature

[1] **Heimburg, T.** (2007). *Thermal Biophysics of Membranes.* WILEY VCH.

[2] **Singer, S. J.** and **G. L. Nicolson** (1975). The Fluid Mosaic Model of the Structure of Cell Membranes. *Science720-731* 1:720–731.

[3] **Cotterill, R. J. M.** (2002). *Biophysics: An Introduction.* Wiley.

[4] **Heimburg, T.** and **D. Marsh** (1993). Investigation of Secondary and Tertiary Structural Changes of Cytochrome c in Complexes with Anionic Lipids Using Amide Hydrogen Exchange Measurements: An FTIR Study. *Biophysical journal* 65:2408–2417.

[5] **Heimburg, T.** and **R. L. Biltonen** (1994). Thermotropic behavior of dimyristoylphosphatidylglycerol and its interaction with cytochrome c. *Biochemistry* 33:9477–9488.

[6] **Oellerich, S.**, **S. Lecomte**, **M. Paternostre**, **T. Heimburg** and **P. Hildebrandt** (2004). Peripheral and integral binding of Cytochrome c to Phospholipids Vesicles. *J. Phys. Chem.* 108:3871–3878.

[7] **Heimburg, T.** and **A. D. Jackson** (2005). On soliton propagation in biomembranes and nerves. *Proc. Natl. Acad. Sci. USA.* 102:9790–9795.

[8] **Hac, A. E.**, **H. M. Seeger**, **M. Fidorra** and **T. Heimburg** (2005). Diffusion in two-component lipid membranes–a fluorescence correlation spectroscopy and monte carlo simulation study. *Biophys J* 88:317–333.

[9] **Mouritsen, O. G.** and **M. Bloom** (1984). Mattress model of lipid-protein interactions in membranes. *Biophys J* 46:141–153.

[10] **Heimburg, T.** and **R. L. Biltonen** (1996). A Monte Carlo simulation study of protein-induced heat capacity changes and lipid-induced protein clustering. *Biophys J* 70:84–96.

[11] **Græsbøll, K.** (2006). Function of Nerves - Action of Anesthetics. *Gamma* 143:27–36.

[12] **Heimburg, T.** and **A. D. Jackson** (2007). The thermodynamics of general anesthesia. *Biophys. J.* 92:3159–3165.

[13] **Hodgkin, A. L.** and **A. F. Huxley** (1952). A quantitative description of membrane current and its application to conduction and excitation in nerve. *J Physiol* 117:500–544.

[14] **Lautrup, B.**, **A. D. Jackson** and **T. Heimburg** (2006). The stability of solitons in biomembranes and nerves. *arXiv:physics/0510106* 1:7.

[15] **Heimburg, T.** and **A. D. Jackson** (2006). On the action potential as a propagating density pulse and the role of anesthetics. *Biophys.* 2:57–78.

[16] *http://en.wikipedia.org/wiki/Infrared spectroscopy.*

[17] **Pedersen, S.** and **B. Ramussen** (2004). *Spektroskopi - Molekylernes fingeraftryk.* Kemi Forlaget, 2 edition.

[18] *http://en.wikipedia.org/wiki/Infrared spectroscopy correlation table.*

[19] **Kittel, C.** and **H. Kroemer** (2002). *Thermal Physics.* Freeman.

[20] **Heimburg, T.** and **D. Marsh** (1994). Protein surface-distribution and protein-protein interactions in the binding of peripheral proteins to charged lipid membranes. *Biophys. J.* 68:536–546.

[21] **Ivanova, V.** and **T. Heimburg** (2001). A histogram method to obtain heat capacity in lipid monolayers, curved bilayers and membranes containing peptides. *Phys. Rev.* 63:1914–1925.

[22] **Ivanova, V. P.** (2000). *Theoretical and experimental study of protein-lipid interactions.* Ph.D. thesis, University of Göttingen.

[23] **Heimburg, T.** (2003). Coupling of chain melting and bilayer structure: domains, rafts, elasticity and fusion. *Book chapter in: Planar lipid bilayers and their applications. H.T. Tien and A. Ottova-Leitmannova* :269–293.

[24] **Heimburg, T.** and **D. Marsh** (1996). Thermodynamics of the interaction of proteins with lipid membranes. *In 'Biologica membranes - A molecuar perspective computation and experiment'. B. Roux and K.M. Merz* :405–461.

Appendix

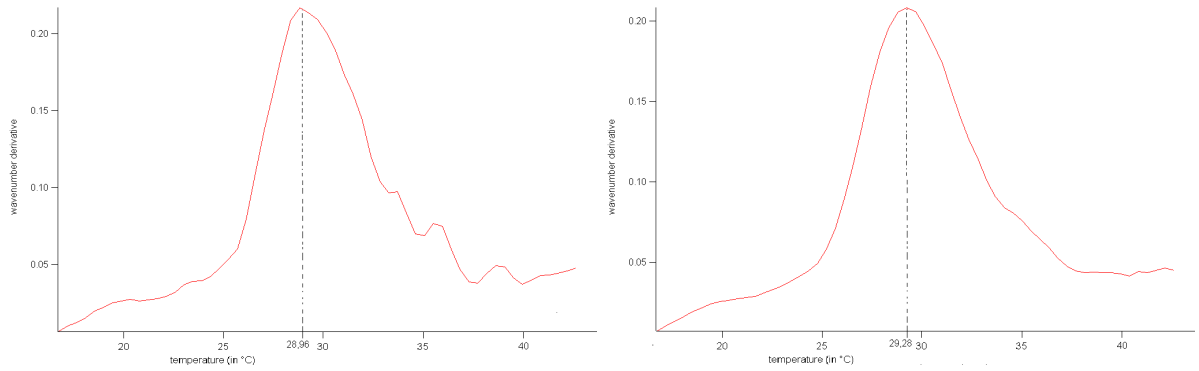

Figure 22: DMPG ($75mM$) with cytochrome c
Left: $n = 2$. Right $n = 4$

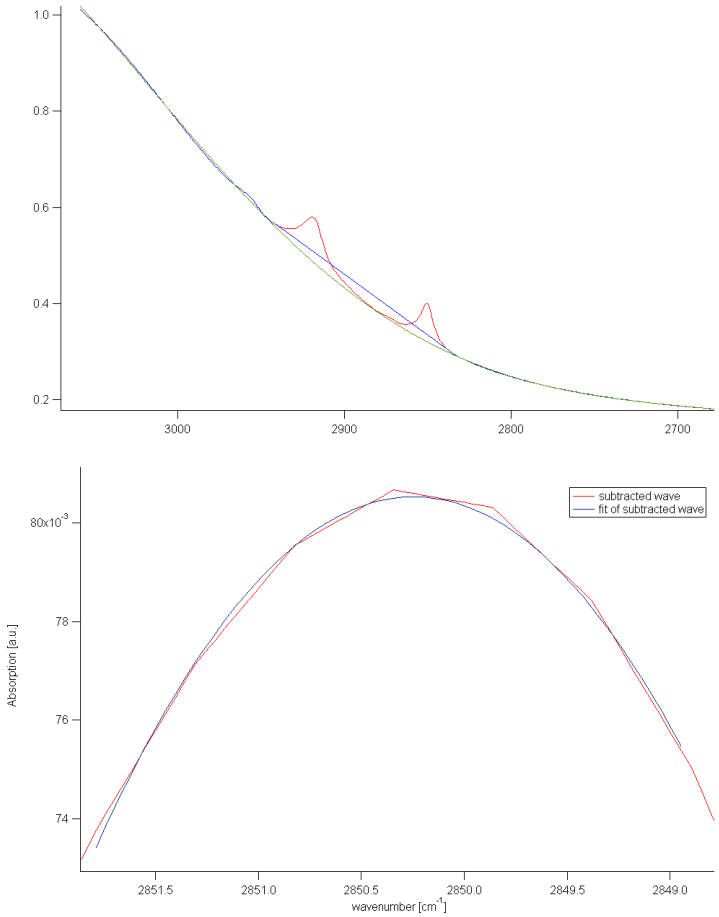

Figure 23: Larger pictures of the baselinecorrection and the peakdetermination